RSC Advances

COMMUNICATION

View Article Online
View Journal | View Issue

Cite this: *RSC Adv.*, 2016, **6**, 102979

Received 26th September 2016
Accepted 21st October 2016

DOI: 10.1039/c6ra23882c

www.rsc.org/advances

Synthesis of push–pull porphyrin dyes with dimethylaminonaphthalene electron-donating groups and their application to dye-sensitized solar cells†

Maryam Adineh,[a] Pooya Tahay,[a] Wei-Kai Huang,[b] Hui-Ping Wu,[b] Eric Wei-Guang Diau*[b] and Nasser Safari*[a]

Two new donor–π-bridge–acceptor zinc porphyrins with dimethylaminonaphthalene electron donating moieties, coded T1 and T2, were synthesized and used as sensitizers in dye sensitized solar cells (DSSCs). Both dyes showed excellent photovoltaic properties with power conversion efficiencies of 8.0 and 9.6% for T1 and T2 respectively, for which the device performance of T2 dye is superior to that of N719 dye.

Dye sensitized solar cells (DSSCs) are third generation solar cells which have attracted much attention because of their low prices, flexibility, low weight, short energy payback times compared with conventional solar cells. A typical DSSC is composed of photoanode, electrolyte and counter electrode. Photoanode is generally made of a semiconductor and sensitizer (dye molecules) on transparent conducting oxide (TCO) substrate; therefore dye plays a crucial role in DSSCs applications.[1] Ruthenium polypyridyl sensitizers have been widely studied in past two decades.[2–7] Broad absorption spectrum through metal-to-ligand charge transfer (MLCT), long exciton lifetime, and long-term chemical stability make them very efficient for DSSC applications. However, many factors such as the high cost of noble metal ruthenium, the requirement for careful synthesis, difficult purification steps and low molar extinction coefficients and so on, limit ruthenium polypyridyl complexes to be uses in DSSC applications.[8] To solve these problems, many researchers were seeking for alternative sensitizers. Porphyrins and their derivatives have attracted remarkable attentions as sensitizers for DSSCs by virtue of their high molar extinction coefficients, ease of modification, photochemical stability and low toxicity as a promising alternative to replace for the ruthenium polypyridyl complexes.[9–17] Considerable breakthrough has been made in the past few years and a record efficiency as high as 13% has been achieved by molecular engineering methodology based on porphyrin SM315 and a cobalt(II/III) redox electrolyte.[15] Similar to the structures of the most organic dyes,[18–20] the porphyrin dyes are designed according to basic structures of donor–π-conjugated bridge–acceptor (simplified as D–π–A) which are beneficial to intramolecular electron transportation.[8,21–24] Most of highly efficient porphyrin sensitizers have such a structural design.[13,15,17,25–31] It is known that the photovoltaic performance of certain planar porphyrin dyes might be further improved by decreasing the degree of dye aggregation.[32] Lin *et al.* designed porphyrin derivatives with long alkoxyl for less dye aggregation and increasing the solubility of chromophore.[14] Inspiring by these works we designed two new D–π–A porphyrins, coded T1 and T2, with dimethylamino naphthalene donor moiety and long alkoxy chain, as sensitizers for DSSCs. To determine the potential energy levels, cyclic voltammetry, differential pulse voltammetery, UV-vis and fluorescence spectroscopy were used. To investigate application of these sensitizers in DSSCs, cells were fabricated using these dyes to compare with the N719 dye. The current–voltage characteristics are provided for the DSSCs with the synthesized photosensitizers. The IPCE action spectra also were taken for cells. To obtain further evidences on frontier orbitals of these dyes, density functional theory (DFT) calculations were carried out. We found that the device made of T2 dye attained power conversion efficiency (PCE) 9.6%, which is superior to that of the N719 device due to the greater light-harvesting ability for the T2 dye than for the N719 dye.

Result and discussion

The molecular structures of porphyrin T1 and T2 are presented in Scheme 1. To reduce the charge recombination reaction induced by molecule aggregation, long alkoxyl chains are attached to porphyrin meso phenyls. As shown in Scheme 1, the only difference for the two porphyrins structures is the triple

[a]*Department of Chemistry, ShahidBeheshti University, Evin, 1983963113 Tehran, Iran. E-mail: n-safari@sbu.ac.ir; Tel: +98-21-2990-2886*

[b]*Department of Applied Chemistry and Institute of Molecular Science, National Chiao Tung University, Hsinchu 300, Taiwan. E-mail: diau@mail.nctu.edu.tw; Fax: +886-3-572-3764; Tel: +886-3-513-1524*

† Electronic supplementary information (ESI) available. See DOI: 10.1039/c6ra23882c

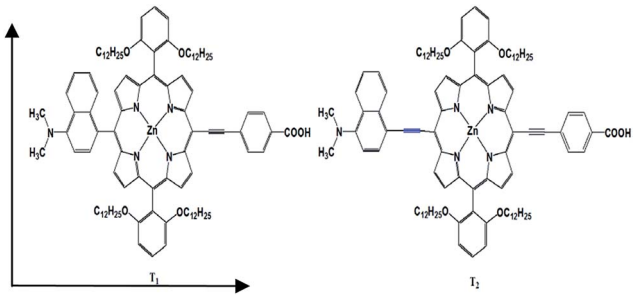

Scheme 1 The molecular structures of porphyrin T1 and T2.

bond between electron donor moiety and porphyrin core. The detailed synthetic procedure for preparing T1 and T2 porphyrins is described in the ESI.†

Fig. 1 displays UV-vis spectra of T1 and T2 in ethanolic solution. As expected, the absorption of T2 ($\lambda_{max} = 453$ nm, $\varepsilon = 2.2 \times 10^5$; 654 nm, $\varepsilon = 3.2 \times 10^4$) is red-shifted and broadened compared to that of T1 ($\lambda_{max} = 445$ nm, $\varepsilon = 2.7 \times 10^5$; 575 nm, $\varepsilon = 1.0 \times 10^4$; 627 nm, $\varepsilon = 1.8 \times 10^4$) due to elongation of π system.[33] A distinct difference in the spectra of the two dyes is the redshift and increase in molar absorptivity of the lowest-energy Q-band for T2. The increased conjugation along the *x*-axis of T2 strongly shifted absorbance from the Q_x transition to produce a maximum at 654 nm. The significant increase in molar absorption coefficient is accordant with the greater oscillator strength of the Q_x transition from increased *x*-axis polarizability within the T2 upon introduction of the acetylene unit.[15]

Fig. 2 shows the fluorescence spectra of two porphyrins. The fluorescence bands of both dyes show the mirror images of the corresponding Q bands, inferring that the gap between vibrational energy levels for the ground and excited states are similar, and the same transitions are desirable for both absorption and emission.[27] The fluorescent maximum of T2 is also red-shifted by 30 nm with respect to that of T1.

The oxidation and reduction potentials of the two dyes were determined by means of cyclic voltammetry (CV). The electrochemical data (Fig. S1†) are summarized in Table 1. T2 showed two oxidation waves at half-wave potential ($E_{1/2}$) = +0.94 and +1.44 V and two reduction waves at half-wave potential ($E_{1/2}$) = −0.51 and −1.03 V *versus* normal hydrogen electrode (NHE). The oxidation values are higher and reduction values are lower than the corresponding potentials of T1 (Table 1). These results indicate that T2 is more difficult to reduce and more difficult to oxidize than T1 which means T2 has a stable structure and has less tendency to be oxidized or reduced. The HOMO and LUMO energy levels for T2 (−5.34 eV and −3.34 eV respectively) are stabilized compared to HOMO and LUMO energy levels for T1 (−5.1 eV and −3.06 eV).

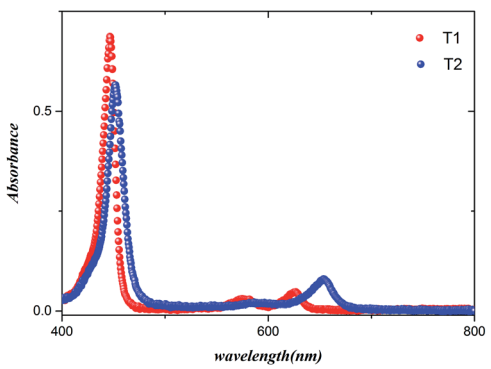

Fig. 1 UV-vis spectra of T1 and T2 in ethanolic solution (0.5 mM).

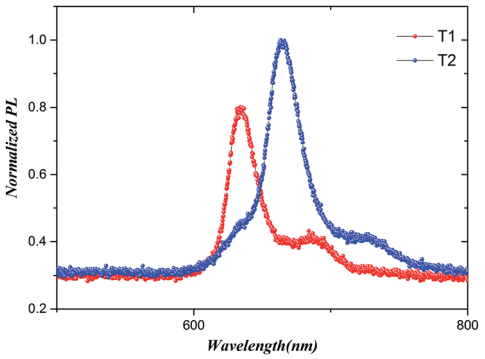

Fig. 2 Fluorescence spectra of T1 and T2 in ethanolic solution (0.5 mM) at 460 nm excitation wavelength.

To gain further insight into the molecular properties, DFT calculations for T1 and T2 were carried out at the B3LYP/6-31G level. The calculated structures do not show negative frequencies, inferring that the optimized geometries are in the global energy minima. Fig. 3 shows the frontier molecular orbitals of each porphyrin. Mizuseki *et al.* proposed that the charge transport was connected with the spatial distribution of the frontier orbitals.[34] For efficient charge transfer the HOMO should be localized in the donor moiety and the LUMO in the acceptor moiety.[35] As shown in Fig. 3, electron distribution of T1 porphyrins, in the HOMO is mostly over the porphyrin core and acetylene bond and there is little distribution on electron donor moiety which is likely due to the fact that the dimethylamino naphthalene is perpendicular to the porphyrin core (dihedral angle = 84°) and do not contribute to electron distributions. As displayed in Fig. 3 on the case of T2 porphyrin naphthalene moiety is planar with porphyrin core the HOMO and is mostly localized over the donor (dimethylaminonaphthalene) and macrocycle moieties; however, the LUMO is populated largely on the macrocycle and the acceptor moieties (π-spacer and carboxyl acid). It is well known that the electron density distribution of LUMO around an anchoring group, affect the electronic coupling between the excited adsorbed dye and 3d orbital

Table 1 The electrochemical data of T1 and T2

Dye	$E_{ox}(1)$	$E_{ox}(2)$	$E_{red}(1)$	$E_{red}(2)$	E_{HOMO}	E_{LUMO}	E_g[a]
T1	+0.69	+0.98	−0.42	—	−5.2	−3.16	2.03
T2	+0.94	+1.44	−0.51	−1.03	−5.44	−3.44	2.00

[a] Estimated from the intersection wavelengths of the normalized UV-vis absorption and the fluorescence spectra.

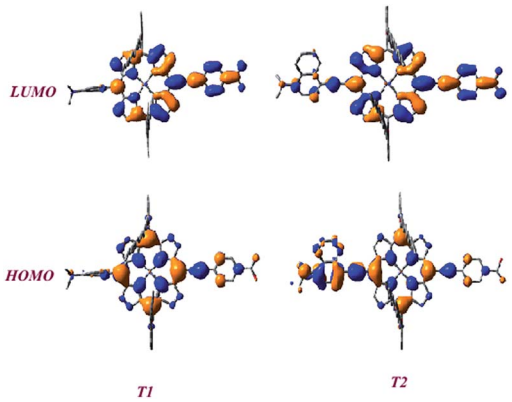

Fig. 3 Frontier molecular orbitals of T1 and T2.

of TiO_2.[36] For both of our studied porphyrins there is noticeable electron distribution around anchoring group at LUMO energy level.

By using of tetrahydrofurane and ethanol (volume ratio 4 : 1) solvent mixture in the presence of cheno acid, T1 and T2 porphyrins were sensitized onto a bilayer (active layer 7.5 μm + scattering layer 5.0 μm) titania film to act as a working electrode. These porphyrins were evaluated in DSSC devices in combination with iodine-based electrolyte.

The difference between the redox potential of I^-/I_3^- and HOMO energy level is given by ΔE. To have fast electron transfer and dye regeneration, ΔE must be positive;[37,38] HOMO energy levels are −5.2 and −5.44 for T1 and T2, respectively; considering that I^-/I_3^- electrolyte potential is −4.85 eV,[39] the differences between electrolyte and HOMO energy level (ΔE) are 0.35 and 0.57 for T1 and T2, respectively. These results show that both of T1 and T2 dyes have sufficient thermodynamic driving force for dye regeneration. On the other hand, electron injection appears to be energetically favorable from the first excited state (LUMO) of both T1 and T2 when compared to the conduction band of TiO_2 because the LUMO energy levels are higher than that of the TiO_2 conduction band ($E_{CB} = -4.0$ eV) to make efficient electron transfer from the dye excited state into the TiO_2 conduction band.

The current–voltage (J–V) characteristics and the corresponding action spectra of incident photons to electrons conversion efficiency (IPCE) of the devices are shown in Fig. 4 and 5 respectively. Detailed photovoltaic parameters such as open circuit voltage (V_{OC}), short circuit photocurrent density (J_{SC}), filling factor (FF) and power conversion efficiency (η) for these dyes under AM 1.5 G one-sun illumination are summarized in Table 2. The higher efficiency as well as short circuit photocurrent density (J_{SC}) for T2 maybe ascribed to its extended π-system which results in more efficient light harvesting ability for the T2 dye than for the T1 dye. The V_{OC} values show the positive shift of the TiO_2 Fermi level in the cell made by T2. This could be because of more dye aggregation due to more planar structure for T2 than for T1. It is well known that dye aggregation and charge recombination can be efficiently reduced for nonplanar and distorted dyes, also the conjugation extension may bring out dye aggregation.[40,41]

The IPCEs for DSSCs based on two dyes are presented in Fig. 5. As shown in Fig. 5, the IPCE action spectra follow the corresponding UV-visible absorption spectra of the two porphyrins. Both dyes show broad IPCE spectra in the visible region. Despite large gap between the Soret and the Q bands of the absorption spectra of porphyrins (Fig. 1), this feature is not noticeable in the IPCE spectra because the effect of light scattering by TiO_2 (ref. 42) shows the whole IPCE spectra with a broad-band feature. J_{SC} calculated from integration of the IPCE values are 17.1 and 21.2 for T1 and T2 respectively showing that there are less than 5% mismatch with experimental values in both cases. The IPCE spectrum of device made by T1 displays photocurrent responses with maximum efficiency of almost 100% at 450 nm but the IPCE spectrum of device made by T2 slightly less than those of the T1 device at this wavelength that could be the extinction coefficient of the Soret band with is higher for T1 than for T2. In comparison with T1, the insertion of an ethynylene bridge in T2 red shifted the onset wavelength of photocurrent response from 730 to 750 nm, resulting in an increase of J_{SC} from 16.6 to exceeding 20 mA cm^{-2}.

In conclusion, two new porphyrins, T1 and T2, with dimethylaminonaphthalene electron donating moiety were designed and synthesized for dye sensitized solar cells. We characterized the photophysical and electrochemical properties of the two dyes and investigated their photovoltaic performance. We found that power conversion efficiency of the T2 device is greater than the T1 device. The higher efficiency observed for T2 maybe ascribed to a better extended π-system which results in more efficient light harvesting ability for the T2 dye than for the

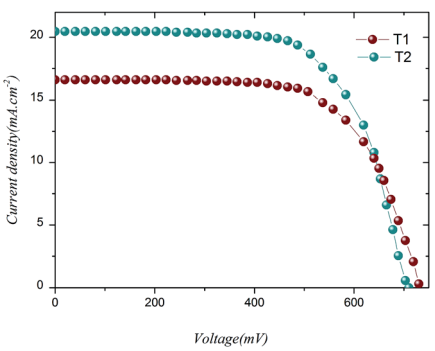

Fig. 4 The current–voltage (J–V) characteristics of T1 and T2.

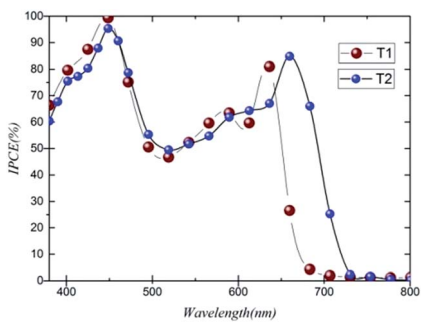

Fig. 5 The IPCE action spectra for DSSCs based on T1 and T2.

Table 2 Photovoltaic parameters of T1 and T2[a]

Dye	V_{OC} (mV)	J_{SC} (mA cm^{-2})	Fill factor (%)	Efficiency (%)
T1	730 (720 ± 15)	16.6 (16.7 ± 0.1)	67 (66 ± 2)	8.1 (7.9 ± 0.2)
T2	712 (710 ± 10)	20.4 (20.3 ± 0.1)	66 (66 ± 2)	9.6 (9.4 ± 0.2)
N719	720 (720 ± 10)	19.4 (19.4 ± 0.1)	65 (66 ± 1)	9.1 (9 ± 0.1)

[a] Values given are the photovoltaic parameters for which the highest efficiency was observed. The average value from eight independent experiments is shown in parenthesis in each case.

T1 dye. The V_{OC} values of cells have the reversed trend (T1 > T2), and this could be due to dye aggregation for which T2 is more significant than T1 due to the molecular structure, for which T2 is more planar than T1. However, the T2 device exhibited a great performance with PCE 9.6%, which is superior to that of the N719 device (9.1%) fabricated under the same experimental conditions.

Acknowledgements

This work was supported by ShahidBeheshti University Research Affaires and National Chiao Tung University (NCTU).

Notes and references

1 A. Hagfeldt, G. Boschloo, L. Sun, L. Kloo and H. Pettersson, *Chem. Rev.*, 2010, **110**, 6595–6663.
2 B. O'Regan and M. Gratzel, *Nature*, 1991, **353**, 737–740.
3 M. K. Nazeeruddin, P. Pechy and M. Gratzel, *Chem. Commun.*, 1997, 1705–1706.
4 R. Argazzi, C. A. Bignozzi, G. M. Hasselmann and G. J. Meyer, *Inorg. Chem.*, 1998, **37**, 4533–4537.
5 L. Zhang, Y. Yang, R. Fan, P. Wang and L. Li, *Dyes Pigm.*, 2012, **92**, 1314–1319.
6 H. Shahroosvand, F. Nasouti and A. Sousaraei, *Dalton Trans.*, 2014, **43**, 5158–5167.
7 M. Ameri and E. Mohajerani, *RSC Adv.*, 2015, **5**, 92690–92706.
8 J. Chen, S. Ko, L. Liu, Y. Sheng, H. Han and X. Li, *New J. Chem.*, 2015, **39**, 2889–2900.
9 M. K. Nazeeruddin, R. Humphry-Baker, D. L. Officer, W. M. Campbell, A. K. Burrell and M. Grätzel, *Langmuir*, 2004, **20**, 6514–6517.
10 W. M. Campbell, K. W. Jolley, P. Wagner, K. Wagner, P. J. Walsh, K. C. Gordon, L. Schmidt-Mende, M. K. Nazeeruddin, Q. Wang and M. Grätzel, *J. Phys. Chem. C*, 2007, **111**, 11760–11762.
11 Y. Liu, N. Xiang, X. Feng, P. Shen, W. Zhou, C. Weng, B. Zhao and S. Tan, *Chem. Commun.*, 2009, 2499–2501.
12 Y.-C. Chang, C.-L. Wang, T.-Y. Pan, S.-H. Hong, C.-M. Lan, H.-H. Kuo, C.-F. Lo, H.-Y. Hsu, C.-Y. Lin and E. W.-G. Diau, *Chem. Commun.*, 2011, **47**, 8910–8912.
13 A. Yella, H. W. Lee, H. N. Tsao, C. Yi, A. K. Chandiran, M. K. Nazeeruddin, E. W. G. Diau, C. Y. Yeh, S. M. Zakeeruddin and M. Grätzel, *Science*, 2011, **334**, 629–634.
14 C.-L. Wang, C.-M. Lan, S.-H. Hong, Y.-F. Wang, T.-Y. Pan, C.-W. Chang, H.-H. Kuo, M.-Y. Kuo, E. W.-G. Diau and C.-Y. Lin, *Energy Environ. Sci.*, 2012, **5**, 6933–6940.
15 S. Mathew, A. Yella, P. Gao, R. Humphry-Baker, B. F. Curchod, N. Ashari-Astani, I. Tavernelli, U. Rothlisberger, M. K. Nazeeruddin and M. Grätzel, *Nat. Chem.*, 2014, **6**, 242–247.
16 H.-H. Chou, K. S. K. Reddy, H.-P. Wu, B.-C. Guo, H.-W. Lee, E. W.-G. Diau, C.-P. Hsu and C.-Y. Yeh, *ACS Appl. Mater. Interfaces*, 2016, **8**, 3418–3427.
17 T. Higashino and H. Imahori, *Dalton Trans.*, 2015, **44**, 448–463.
18 Z. Yao, M. Zhang, H. Wu, L. Yang, R. Li and P. Wang, *J. Am. Chem. Soc.*, 2015, **137**, 3799–3802.
19 S. M. Feldt, E. A. Gibson, E. Gabrielsson, L. Sun, G. Boschloo and A. Hagfeldt, *J. Am. Chem. Soc.*, 2010, **132**, 16714–16724.
20 G. Zhang, H. Bala, Y. Cheng, D. Shi, X. Lv, Q. Yu and P. Wang, *Chem. Commun.*, 2009, **16**, 2198–2200.
21 D. Arteaga, R. Cotta, A. Ortiz, B. Insuasty, N. Martin and L. Echegoyen, *Dyes Pigm.*, 2015, **112**, 127–137.
22 W. M. Campbell, A. K. Burrell, D. L. Officer and K. W. Jolley, *Coord. Chem. Rev.*, 2004, **248**, 1363–1379.
23 T. Bessho, S. M. Zakeeruddin, C.-Y. Yeh, E. W.-G. Diau and M. Grätzel, *Angew. Chem., Int. Ed.*, 2010, **49**, 6646–6649.
24 C.-P. Hsieh, H.-P. Lu, C.-L. Chiu, C.-W. Lee, S.-H. Chuang, C.-L. Mai, W.-N. Yen, S.-J. Hsu, E. W.-G. Diau and C.-Y. Yeh, *J. Mater. Chem.*, 2010, **20**, 1127–1134.
25 H.-P. Wu, Z.-W. Ou, T.-Y. Pan, C.-M. Lan, W.-K. Huang, H.-W. Lee, N. M. Reddy, C.-T. Chen, W.-S. Chao, C.-Y. Yeh and E. W.-G. Diau, *Energy Environ. Sci.*, 2012, **5**, 9843–9848.
26 C.-L. Wang, J.-Y. Hu, C.-H. Wu, H.-H. Kuo, Y.-C. Chang, Z.-J. Lan, H.-P. Wu, E. Wei-Guang Diau and C.-Y. Lin, *Energy Environ. Sci.*, 2014, **7**, 1392–1396.
27 C.-L. Wang, M. Zhang, Y.-H. Hsiao, C.-K. Tseng, C.-L. Liu, M. Xu, P. Wang and C.-Y. Lin, *Energy Environ. Sci.*, 2016, **9**, 200–206.
28 J. Luo, M. Xu, R. Li, K.-W. Huang, C. Jiang, Q. Qi, W. Zeng, J. Zhang, C. Chi, P. Wang and J. Wu, *J. Am. Chem. Soc.*, 2014, **136**, 265–272.
29 T. Higashino, Y. Fujimori, K. Sugiura, Y. Tsuji, S. Ito and H. Imahori, *Angew. Chem., Int. Ed.*, 2015, **54**, 9052–9056.
30 K. Kurotobi, Y. Toude, K. Kawamoto, Y. Fujimori, S. Ito, P. Chabera, V. Sundström and H. Imahori, *Chem.–Eur. J.*, 2013, **19**, 17075–17081.
31 R. Zong and R. P. Thummel, *J. Am. Chem. Soc.*, 2005, **127**, 12802–12803.
32 L. Luo, C.-J. Lin, C.-Y. Tsai, H.-P. Wu, L.-L. Li, C.-F. Lo, C.-Y. Lin and E. W.-G. Diau, *Phys. Chem. Chem. Phys.*, 2010, **12**, 1064–1071.
33 H. Imahori, T. Umeyama and S. Ito, *Acc. Chem. Res.*, 2009, **42**, 1809–1818.
34 H. Mizuseki, K. Niimura, C. Majumder, R. V. Belosludov, A. A. Farajian, Y. Kawazoe and C. Majumder, *Mol. Cryst. Liq. Cryst.*, 2003, **406**, 11–17.

35 H. Shahroosvand, S. Zakavi, A. Sousaraei and M. Eskandari, *Phys. Chem. Chem. Phys.*, 2015, **17**, 6347–6358.
36 H. Imahori, Y. Matsubara, H. Iijima, T. Umeyama, Y. Matano, S. Ito, M. Niemi, N. V. Tkachenko and H. Lemmetyinen, *J. Phys. Chem. C*, 2010, **114**, 10656–10665.
37 A. Luque and S. Hegedus, *Handbook of Photovoltaic Science and Engineering*, 2011, 2nd edn.
38 J. Lu, H. Li, S. Liu, Y.-C. Chang, H.-P. Wu, Y.-B. Cheng, E. W.-G. Diau and M. Wang, *Phys. Chem. Chem. Phys.*, 2016, DOI: 10.1039/c5cp05658f.
39 G. Boschloo and A. Hagfeldt, *Acc. Chem. Res.*, 2009, **42**, 1819–1826.
40 Y. Wang, X. Li, B. Liu, W. Wu, W. Zhu and Y. Xie, *RSC Adv.*, 2013, **3**, 14780–14790.
41 Y. Xie, Y. Tang, W. Wu, Y. Wang, J. Liu, X. Li, H. Tian and W.-H. Zhu, *J. Am. Chem. Soc.*, 2015, **137**, 14055–14058.
42 S.-L. Wu, H.-P. Lu, H.-T. Yu, S.-H. Chuang, C.-L. Chiu, C.-W. Lee, E. W.-G. Diau and C.-Y. Yeh, *Energy Environ. Sci.*, 2010, **3**, 949–955.